



Estimating Uncertainty and Bias in Deterministic Inversions

John V. Pendrel, Henk J. Schouten, Raphaël Bornard
CGG

Summary

It has become common to use a Bayesian inference procedure as the key interpretation tool for seismic inversions. The results are facies and their probabilities of occurrence derived from the native outcomes of inversions or their derivatives. However, deterministic inversions must have some uncertainties associated with them. Further, due to sub-optimal parameter selection or increasingly thin bedding, biases in the inversion properties can arise. We use a phenomenological approach to model these effects and correct for them in the subsequent Bayesian inference. The results are facies interpretations which account for bias and uncertainties and which will provide increased confidence in reservoir volume estimations.

Introduction

Bayesian inference can be used to infer the probabilities of occurrence of geologic facies from seismic reflection data and in particular, from full-stack and AVO inversions (Pendrel et al., 2006). It is observed that facies when displayed in a cross-plot space defined by inversion outcomes, commonly exhibit a clustering behaviour. This clustering can be described by assigning joint probability density functions (fPDFs) to each facies. Applying Bayes' rule with optional priors provides the probability of occurrence of each of the facies at every location in 3D space. Volumes of the most-probable facies follow immediately. The design of the fPDFs comes initially from well log data but can be augmented by rock physics modeling or any other available information. The cross-plot space need not be restricted to the native outcomes of inversions but can be any derivatives thereof. For example, in unconventional shale plays, Vqtz and Brittleness have been used (Pendrel et al., 2014).

It has been recognized that deterministic seismic inversions, while producing one single set of most-likely reservoir properties, contain inherent uncertainties. These can arise, for example, from random and coherent noise in the seismic data, bandwidth limitations and uncertainty in the estimated angles of incidence and the inversion wavelets. A rigorous approach might be to estimate the uncertainties in each of the inversion inputs and from these, the net uncertainty in the inversion outcomes. Here we take a more phenomenological approach as described below.

Method

The inversion algorithm which we employ makes no use and has no knowledge of any well log information within the seismic band. Notwithstanding the possible construction of low frequency models (LFMs) from logs to complete the low frequency portion of the inversion, we can say that the inversion algorithm is blind to the logs within the seismic band. It then follows that an effective QC is the comparison of the inversions to logs at the well locations. A cross-plot of high-cut filtered logs vs inversion outputs should result in a set of data points clustering along a line with a slope of unity. Any deviation from this slope is an indication of bias. Bias can result, for example, from deficiencies in the inversion parameter settings or as a result of a loss of resolution in thin bed scenarios. Furthermore, it can be variable from one geologic layer to the next. The observation that the data points in the QC cross-plot cluster along the best-fit line rather than lie on it is

an indication of uncertainty. It can arise from several sources, some of which have been described above. We measure the distance of each data point from the best-fit line and use these to construct a residual histogram. To this we fit an Uncertainty PDF (uPDF). When this is done for each of the inversion outputs, the uPDFs are incorporated into the Bayesian facies analysis. The outcomes of inversion are no longer represented by single points in the inversion cross-plot space on which the facies PDFs are defined but by ellipses. Should a bias correction be necessary, then the ellipses are shifted. We recognize the possibility that the uncertainties from associated inversion outputs could be correlated. This would mean that the multi-dimensional uPDFs would be rotated. We have not seen this effect in real data and so do not pursue that notion further here. We also note that the PDFs could be defined through a non-parametric approach which we have also not considered in this writing. The effect of the uPDFs is to add uncertainty to the individual facies probabilities. As the standard deviations of the uPDFs become larger, the probabilities of occurrence of the facies become more similar and the ability to discriminate between them is reduced.

Example

We test the above ideas with a Gulf of Mexico data set. The key horizon is the top of the Green sand which is shown in Figure 1. Below the Green horizon, we recognize both upper and lower Green sandstones. Sharp discontinuities are the results of faulting. Geologically, there is a set of two vertically-stacked deltaic systems of middle Pliocene age. They average about 400 ft. in thickness and are separated by about 500 ft. Within the play area are delta slope deformation, slump-induced turbidites, thin mouth-bed deposits but without the presence of any delta plain facies.

The available seismic consisted of five partial-angle stacks with the maximum angle in the farthest stack being 50 degrees. This was not judged to be sufficient to resolve density with any degree of certainty. A single set of wavelets, one for each partial stack, was obtained by matching elastic synthetics to the seismic at each of the seven available wells. The log sets included full-wave sonic logs over the reservoir interval, facilitating the creation of the AVO wavelets. A simultaneous AVO inversion algorithm (Pendrel et al., 2000) was used to complete the inversions. Low frequency information was supplied to the inversion in the form of facies-based constant trends interactively defined at horizons and hung on structure. The lowest frequencies were further modified using stacking velocity information (Pendrel, 2015).

The results of the relative (no low frequencies) simultaneous inversion are shown in Figure 2 along an arbitrary line passing through all the wells. Band-pass-filtered logs are overlain. The matches are not perfect since the inversion has no prior knowledge of the high frequency component of the logs. The region of interest is the G sand (between the orange arrows) where there is the possibility of hydrocarbon deposits. The P Impedance agreement to wells is good and the Vp/Vs fair.

Figure 3 shows the Facies PDF templates used in the Bayesian inference for the upper and lower G sandstones. Note how the characteristics of the sandstones change in this short time interval. Bias QCs for P Impedance and Vp/Vs are shown in Figure 4 for the upper sandstones. There is considerable scatter (uncertainty) as well as significant bias. These can be seen clearly in the difference histogram plots in Figure 5. Biases of 2.4% and 0.6% exist for P Impedance and Vp/Vs, respectively. Since the modelled uPDFs in Figure 4 are used in the Bayesian analysis, a bias correction is effectively made.

Figures 6 and 7 compare the results of the Bayesian facies classifications when uncertainties and bias were ignored and when they were incorporated. In Figure 6 showing the most-probable facies, there is generally less pay in the bias-corrected versions. Apparently, the small biases in the inversion had resulted in wrongly classifying some wet sandstone as pay. As expected, the Pay probabilities in Figure 7 are reduced generally when uncertainties and bias are taken into account. There is increased confidence in the surviving high probability areas however, since imperfections in the inversion have been corrected.

Conclusions

We have demonstrated that small biases and uncertainties in seismic inversions of only a few percent can significantly affect critical facies identifications. These can be estimated and input to the Bayesian inference procedure on a layer-by-layer basis to correct the inversions and produce faithful facies interpretations. Incorporating uncertainties in the low frequency model away from well control is a matter for our future consideration and any uncertainties therein will add to those described here.

Acknowledgements

The authors wish to thank their colleagues in the CGG GeoSoftware team for their valuable comments and support. Thanks particularly to Peter Mesdag for several insightful conversations.

References

- Pendrel, J., Debeye, H., Pedersen-Tatalovic, R., Goodway, B., Dufour, J., Bogaards, M., Stewart, R., 2000, Estimation and interpretation of P and S Impedance volumes from the simultaneous inversion of P-wave offset data, CSEG Ann. Mtg. Abs.
- Pendrel, J., Mangat, C., Feroci, M., 2006, Using Bayesian inference to compute facies-fluids probabilities, CSEG Ann. Mtg. Abs.
- Pendrel, J., Marini, A.I., 2014, Static models for unconventional reservoirs: a Barnett shale case study, SEG Summer Workshop Abs., San Diego
- Pendrel, J., 2015, Low frequency models for seismic inversions: strategies for success, SEG Ann. Mtg. Abs.

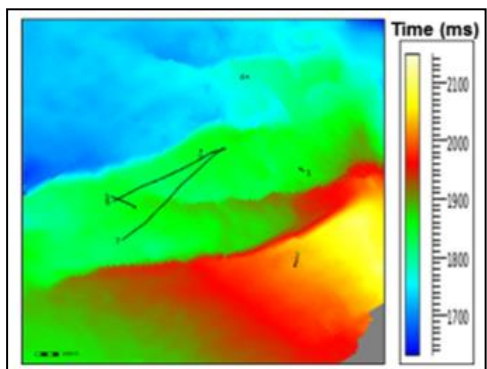


Figure 1: Project map shows the green horizon and the well locations.

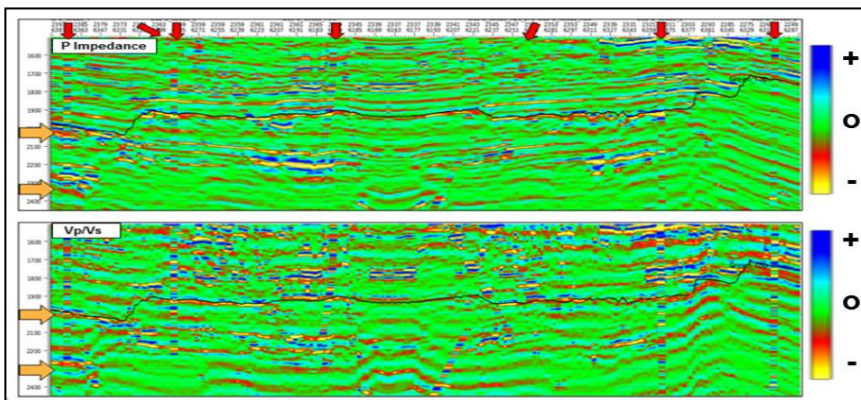


Figure 2: P Impedance and Vp/Vs from a relative inversion (no low frequencies). Band-pass-filtered logs have been overlain at the well locations (red arrows). The inversion algorithm was blind to the wells in the seismic band.

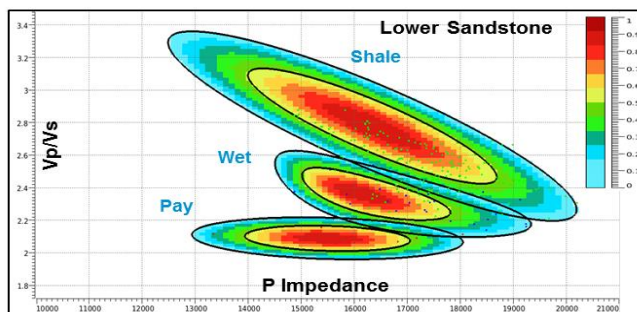
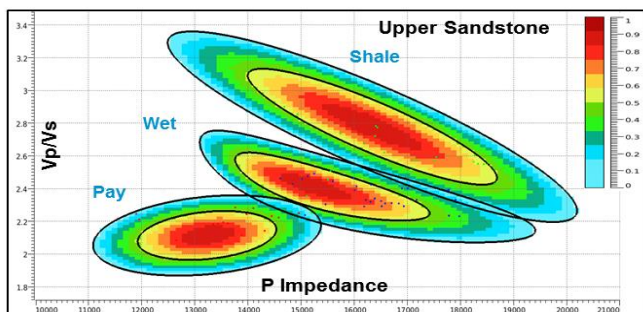


Figure 3: Bayesian facies analysis templates for the upper G sandstone (left) and the lower G sandstone (right). For each fPDF, two standard deviations are plotted.

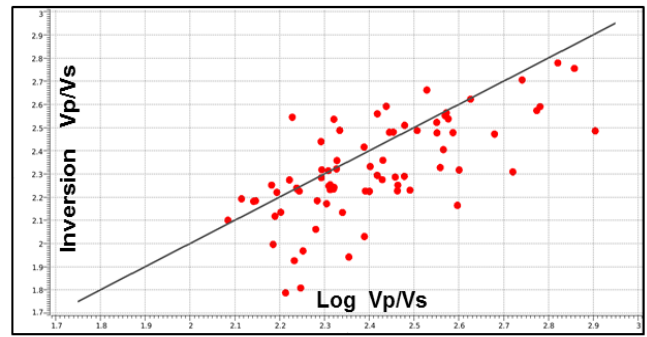
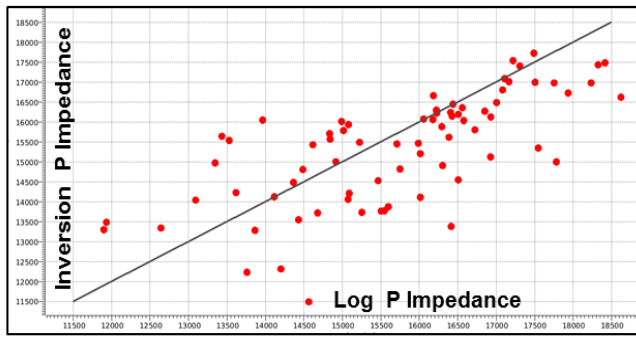


Figure 4: Cross-plots of properties from inversion with their high-cut-filtered log counterparts indicate deviations from a one-to-one line and therefore, bias. There is also significant scatter representing uncertainty in the inversion results. These data are from the upper Green sandstone. Similar plots were made for the lower sandstones.

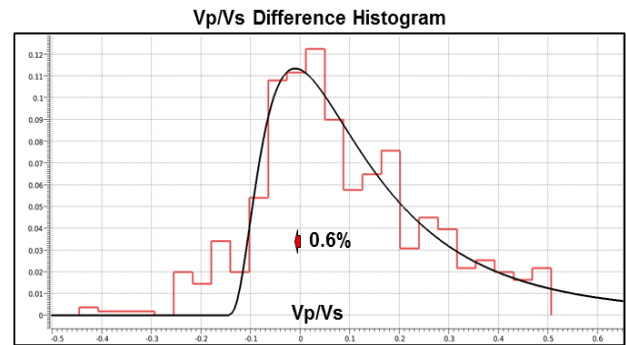
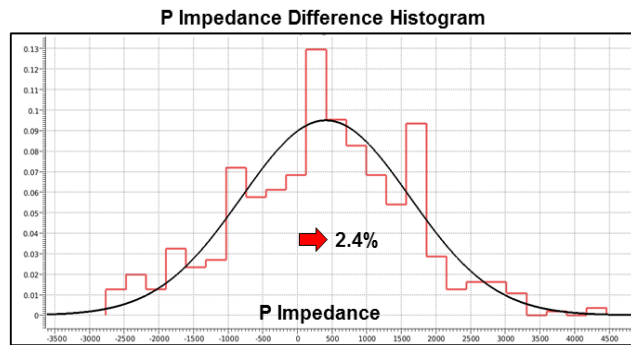


Figure 5: The two histogram plots measure and model the biases and uncertainties corresponding to P Impedance and Vp/Vs. The model uPDFs (black lines) are used in the Bayesian inference procedure to correct the facies identifications. The results shown are for the upper Green sandstones. Similar plots were made for the lower sandstones.

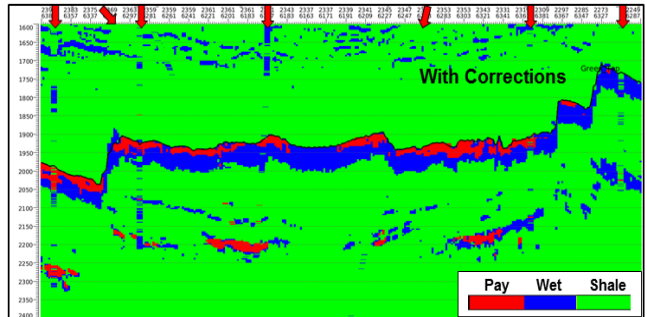
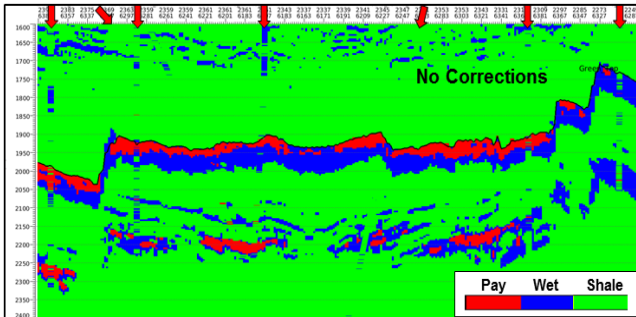


Figure 6: Two versions of the most-probable facies are shown, corresponding to no corrections (left) and with both bias and uncertainty corrections (right). Apparently, some wet facies were misclassified as pay in the left figure.

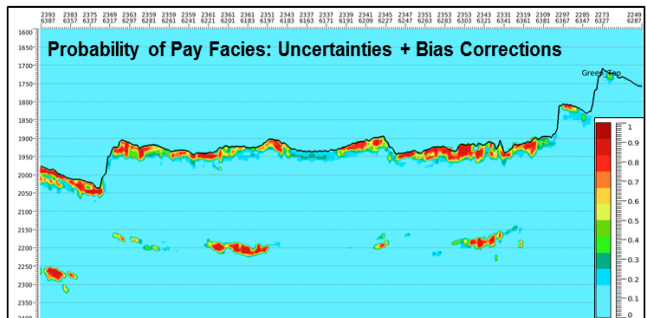
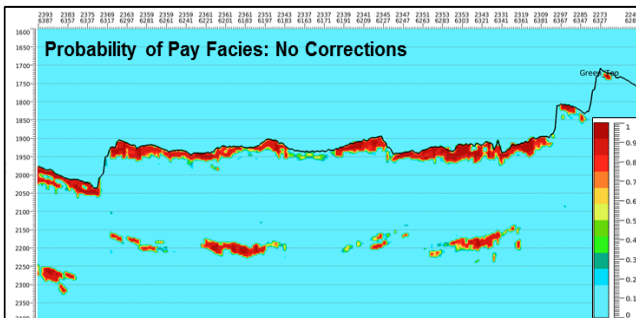


Figure 7: Shown are the probabilities of occurrence of the pay facies corresponding to the most-probable facies figures above. The probabilities of Pay have been reduced due to inversion uncertainty or where the facies had been incorrectly classified.